Journal of Agricultural Engineering

https://www.agroengineering.org/

Design and development of an anti-drift device for maize (*Zea mays* L.)-soybean (*Glycine max* (L.) Merr. intercropping systems

Li Jiang,[1,2] Yuehan Li,[1] Wei Lu,[1,2] Guanqun Wang[1,2,3]

[1]School of Agricultural Engineering, Jiangsu University, Zhenjiang
[2]High-tech Key Laboratory of Agricultural Equipment and Intelligence of Jiangsu Province, Jiangsu University, Zhenjiang
[3]School of Automotive Engineering, Yancheng Institute of Technology, Yancheng, China

Corresponding author: Guanqun Wang, School of Automotive Engineering, Yancheng Institute of Technology, 111 Zhuhui Road, Tinghu District, Yancheng 224051, China. E-mail: wgq1994@ycit.edu.cn

Please cite this article as doi: 10.4081/jae.2026.1874

Submitted: 8 June 2025
Accepted: 27 April 2026

Design and development of an anti-drift device for maize (*Zea mays* L.)-soybean (*Glycine max* (L.) Merr. intercropping systems

Li Jiang,[1,2] Yuehan Li,[1] Wei Lu,[1,2] Guanqun Wang[1,2,3]

[1]School of Agricultural Engineering, Jiangsu University, Zhenjiang
[2]High-tech Key Laboratory of Agricultural Equipment and Intelligence of Jiangsu Province, Jiangsu University, Zhenjiang
[3]School of Automotive Engineering, Yancheng Institute of Technology, Yancheng, China

Corresponding author: Guanqun Wang, School of Automotive Engineering, Yancheng Institute of Technology, 111 Zhuhui Road, Tinghu District, Yancheng 224051, China. E-mail: wgq1994@ycit.edu.cn

Contributions: all the authors made a substantive intellectual contribution, read and approved the final version of the manuscript and agreed to be accountable for all aspects of the work.

Conflict of interest: the authors declare that they have no known competing financial interests or personal relationships that could have appeared to influence the work reported in this paper.

Acknowledgments: this research was funded by the Priority Academic Program Development of Jiangsu Higher Education Institutions (grant number: PAPD-2023-87) and project of High-tech Key Laboratory of Agricultural Equipment and Intelligence of Jiangsu Province(No. MAET202323)

Abstract

Spray drift can severely reduce crop yields in maize (*Zea mays* L.)-soybean (*Glycine max* (L.) Merr.) strip intercropping systems. A novel hood structure for a spray unit was developed to mitigate herbicide drift. By integrating the structural stability of trapezoidal profiles with the aerodynamic advantages of arcuate shapes, a hooded spray unit was designed. A three-factor, three-level orthogonal experiment was conducted to optimize key structural parameters.. Analysis of variance revealed that opening width (L=1200mm) and hood height (H=650mm) significantly influenced drift rate, while inclination angle (θ=80°) had a lesser effect. Simulation results showed that the optimized hood reduced droplet mass-center displacement by up to 21.89 cm and lowered drift rate by 27.4% compared to a without-hood sprayer. Comparative analyses of four hood designs further confirmed

the superior performance of the proposed structure in promoting deposition and suppressing drift. Prototype experiments on an intercropping-specific boom sprayer show droplet deposition densities on non-target strips remained below 2.1 droplets cm^{-2}, demonstrating effective isolation. These findings indicate that the novel hood design meets agronomic requirements for maize-soybean intercropping and offers a practical solution for precision weed control with reduced environmental impact.

Key words: spray hood; computational fluid dynamics; drift rate; application technology.

Introduction

Soybean (*Glycine max* (L.)'s nutritional value is globally recognized. However, balancing high yields with sustainable development remains a major challenge for agriculture (Padalkar *et al.*, 2023). Maize (*Zea mays* L.)-soybean strip intercropping enhances air circulation, reduces light loss, and improves stress tolerance (Wu *et al.*, 2023). By integrating plant-soil feedback technology, intercropping systems maintain soil health and ensure safe production (Kama *et al.*, 2024). Compared with monoculture, this system improves overall performance by approximately 30%, increases land-use efficiency, promotes crop symbiosis (Li *et al.*, 2020) and does not increase the energy demand of the operation (Cortez *et al.*, 2018). Adopting this pattern therefore reduces pressure on soybean production. Management of pests, diseases, and weeds is critical for achieving high and stable yields in maize-soybean strip intercropping (Dong *et al.*, 2025). Maize, a grass species, and soybean, a broadleaf species, require different herbicides. Moreover, spray drift can severely reduce final yields. Existing plant-protection implements for strip intercropping are merely simple modifications of conventional equipment. They fail to support mechanized, efficient production and exhibit high phytotoxicity, low efficiency, and poor adaptability (Moore *et al.*, 2022).

Covered-spray application installs isolation hoods to separate the crop from the external environment, creating a semi-enclosed spraying zone that effectively reduces droplet drift in intercropping systems (Li *et al.*, 2023). Ozkan were the first to evaluate nine mechanical shielding devices for their ability to reduce droplet loss, using the nozzle-to-droplet center-of-mass distance as the metric under wind-tunnel conditions (Ozkan *et al.*, 1997). The Danish company SKOVHAVE developed hoods in various sizes -initially for strawberry growers and later for other row crops. Willmar Fabrication

produces a hooded sprayer primarily used for sugarcane weed control to limit herbicide drift. Liu *et al.* (2021) designed a conical airflow-based anti-drift device that minimizes vertical drift losses. With the advent of UAV-based spraying systems, similar enclosure structures have been incorporated into multirotor plant-protection drones (Kong *et al*., 2024). Although these studies have generated various hood designs for conventional sprayers, none have specifically analyzed anti-drift performance in strip intercropping systems.

Different types and sizes of hoods can significantly influence spray performance; therefore, they must be selected and optimized for specific field conditions. Accordingly, investigating airflow patterns around and within the hoods and refining their structural design and dimensional parameters are crucial. This approach ensures optimal spray deposition and meets stringent requirements for preventing cross-strip droplet drift during herbicide application in maize-soybean strip intercropping. In this study, CFD simulations were first employed to analyze airflow characteristics and optimize the structural parameters of the hood. Subsequently, prototype experiments were conducted to validate the simulation results and evaluate the anti-drift performance under practical conditions. This combined approach ensures both theoretical analysis and experimental verification.

Materials and Methods

Working principle and structural design of the wind shield

According to previous studies, hoods can adopt either a trapezoidal or an arcuate profile as their primary geometry (Ozkan *et al.*, 1997). In practice, the trapezoidal configuration is widely used for its superior stability and load-bearing capacity. Conversely, the arcuate form, with its streamlined shape, effectively reduces aerodynamic drag and maintains robust performance under strong winds. By integrating the advantages of both designs, a novel hood tailored for strip-intercropping systems was developed (Figure 1). An orthogonal experimental design determined the optimal structural variables of the hood. This method is commonly used in multi-factor, multi-level mechanical design studies and in optimizing agricultural machinery operating parameters (Li *et al.*, 2019; Yu *et al.*, 2023; Liu *et al.*, 2024). Three factors -hood height (H), lower opening width (L), and inclination angle (θ)- were selected at three levels, and a 3^3 orthogonal design was used to determine the optimal combination. Drift rate served as the evaluation metric. Analysis of variance on the drift data pinpointed the optimal factor levels, thus establishing the hood's ideal dimensions.

Numerical simulation model of the hood airflow field

Advances in computational fluid dynamics (CFD) provide a solid theoretical basis for resolving two-phase flow problems (Tang *et al.*, 2017). ANSYS Fluent simulates three-dimensional gas flow and tracks droplet trajectories (Qin *et al.*, 2016; Laguardia *et al.*, 2023). It also quantifies spray performance metrics through numerical calculations and simulation analyses (Baetens *et al.*, 2007; Nuyttens *et al.*, 2017). Compared with costly wind-tunnel experiments and stringent operational requirements, CFD is better suited for designing and optimizing spraying equipment. Tsay used FLUENT (version 2022 R1) to model droplet trajectories and flow-field characteristics for six hood geometries (Tsay *et al.*, 2002).

The experimental study was conducted to validate the effectiveness of the optimized hood structure obtained from the CFD simulations and to assess its performance under practical operating conditions. The airflow field was solved using a pressure-based solver with the SIMPLE algorithm. A second-order upwind scheme was adopted for discretization to improve numerical accuracy.

The Lagrangian Discrete Phase Model (DPM) was employed to simulate droplet motion. Since spraying occurs under ambient temperature conditions, thermal effects were neglected. The airflow was treated as incompressible due to the low operating wind speed, corresponding to a low Mach number condition. Therefore, only the mass and momentum conservation equations were solved, and the energy equation was not considered (Dong *et al.*, 2023). Droplet trajectories are computed using the Euler-Lagrange approach (Tu *et al.*, 2018). The discrete-phase particle motion equation is expressed as follows:

$$\frac{d\mu_p}{dt} = \frac{18\mu C_D R_e}{24\rho_p d_p^2}\left(u - u_p\right) + \frac{g(\rho_p - \rho)}{\rho_p} + \frac{1}{2}\frac{\rho}{\rho_p}\frac{d}{d_t}(u - u_p) \qquad \text{(Eq. 1)}$$

Where:

u_p denotes the velocity of the discrete phase;

μ denotes the dynamic viscosity of the continuous phase;

C_D denotes the drag coefficient;

R_e denotes the relative Reynolds number;

ρ_p denotes the density of the discrete phase;

d_p denotes the diameter of the discrete particles;

g denotes the acceleration due to gravity.

Turbulence effects were modeled using the realizable k-ε model, which is suitable for external flows with complex geometries and has been widely applied in agricultural airflow simulations. The discrete phase was simulated using the Lagrangian Discrete Phase Model (DPM). Droplets were injected at the nozzle outlet using a surface injection method. The droplet size distribution followed a Rosin–Rammler distribution, and their trajectories were calculated considering drag force and gravity. Droplet evaporation, breakup, and coalescence were neglected to simplify the model. The simulations were conducted under transient conditions to capture the time-dependent behavior of airflow and droplet transport. The initial droplet velocity was assumed to be consistent with typical nozzle exit conditions reported in the literature. The characteristic droplet size distribution parameters were selected based on representative flat-fan nozzle spraying conditions. Due to the focus on macroscopic droplet transport and drift behavior, detailed nozzle internal flow characteristics were not explicitly modeled.

In the numerical simulation of the two-phase flow field, droplet evaporation, breakup, and coalescence were neglected, and the droplet size distribution was assumed to follow a Rosin-Rammler distribution. Based on the hood's geometry and dimensions, a computational domain was created in SolidWorks (version 2022) with overall dimensions of 4 m (L) × 2 m (W) × 1.2 m (H). The quadrilateral ABCD face served as the natural wind inlet. The hood was placed 1 m downstream of this inlet, with its lower edge positioned 250 mm above the ground. The resulting three-dimensional airflow field model is shown in Figure 2.

Ambient wind in the three-dimensional fluent domain flows along the positive X-axis. A velocity-inlet boundary condition is applied to the wind-entry face. The flow is treated as incompressible. Wind speed critically affects operational safety and spray performance. According to the Field Operation Specifications for Plant-Protection Machinery, Beaufort scale 3 winds (3.4-5.4 m/s) noticeably disrupt field spraying operations. Therefore, the inlet wind speed was uniformly set to 5 m/s in the CFD simulations. All downstream boundaries were defined as pressure outlets.. Quadrilateral ABCD is the inlet, while ACEG, ABEF, CDGH, and BDGF serve as pressure-outlet boundaries.

Choosing an appropriate solver algorithm enhances CFD efficiency and accuracy. A pressure-based solver with the SIMPLE algorithm was selected under the Solution Methods settings. This solver is well suited for most conventional incompressible flows and offers rapid convergence. Since the airflow driving droplet drift is incompressible, the SIMPLE algorithm was employed. All transport equations are discretized using a second-order upwind scheme (Hu *et al.*, 2021). Airflow field simulations for nine hood geometries were conducted using Fluent. The selected values of inclination angle θ (°), lower opening width L (mm), and height H (mm) for these nine cases are listed in Table 1.

Performance comparison of different hoods

The hood's geometry modifies the local airflow around droplets, promoting rapid deposition onto crops and thus reducing drift. Based on the CFD simulation results, the proposed intercropping hood was compared with three existing drift-control devices used on strip-intercropping sprayers (Figure 3). The anti-drift performance of each configuration was evaluated under the maize–soybean strip intercropping system. Hood (a) comprises two flat panels spaced 1.2 m apart, with a height of 0.8 m and no top cover. Fabricated from 3 mm-thick polyester sheet, it effectively blocks inter-strip droplet drift while minimizing seedling damage and mounts to the spray boom via fasteners and U-shaped connectors (Cui *et al*., 2023).

Hood (b) features a semicircular profile with a 0.6 m radius and a 0.2 m opening height. Originally developed for potato crop protection, it has demonstrated excellent drift-reduction performance in trials (Wei *et al*., 2021).

Hood (c) enhances design (b) by replacing the lower half with two inclined flat panels while retaining a 0.45 m-diameter arc in the upper half. The flat panels incline at 85°; the bottom opening width is 1.2 m; the opening height remains 0.2 m.

Hood (d) represents the novel structure proposed in this study.

Experimental evaluation of anti-drift performance with physical samples

Based on the optimal factor levels identified by the orthogonal design, hood prototypes were fabricated and mounted on a test rig for anti-drift trials. These experiments assessed the hoods' ability to separate two agrochemical formulations under realistic conditions. Separate valves and plumbing

lines were installed for the maize and soybean spray units. During maize-strip drift tests, only the maize spray system was activated, and the soybean system remained off. Conversely, during soybean-strip drift tests, only the soybean spray unit operated. Wind speed during the experiments was measured using a hot-wire anemometer (GM8903; Biaozhi, Shenzhen, China). Spray pressure was monitored using the built-in pressure gauge of the sprayer system.

Artificial plants replaced living crops and were arranged in a 4:2 maize-to-soybean row ratio. Maize simulants were 40 cm tall, and soybean simulants were 25 cm tall. Within each soybean strip, plant spacing alternated at 20 cm, 40 cm, and 20 cm; in the maize strip, spacing was uniformly 40 cm. The inter-row distance between maize and soybean strips was set to 60 cm (Figure 4). The sprayer passed the artificial rows at 3, 4, and 5 km/h to evaluate droplet drift under varying field-operating speeds. Test conditions were as follows: April 26, 2025, 13:00-16:00; Zhenjiang, China; ambient temperature 20-25°C; relative humidity 20%; southeast wind at Beaufort scale 3 (3.4-5.4 m/s).

Although the experiments were conducted under open-field conditions, key environmental parameters, including wind speed, temperature, and relative humidity, were monitored and maintained within a controlled range during the test period. To improve the reliability of the results, each experimental condition was repeated three times, and the average values were used for analysis to reduce random variability. Although minor fluctuations in ambient wind speed and direction were unavoidable under open-field conditions, the overall experimental trends remained consistent. The purpose of the experiments was to validate the relative performance and drift-reduction capability of the proposed hood, rather than to replicate a fully controlled flow field. Therefore, the experimental results are considered sufficient to support the effectiveness of the proposed design and to provide practical validation of the CFD findings.

Because droplet coverage on water-sensitive paper (WSP) during drift tests is very low (Ahmad *et al*., 2022) and WSP exhibits an underestimation of fine droplets (da Cunha *et al.*, 2019), this experiment adopts droplet deposition density as the evaluation metric. Droplet deposition density, defined as the number of droplets deposited per unit area of crop surface, is calculated as follows:

$$D = \frac{n}{S} \quad \text{(Eq. 2)}$$

Where:

D-droplet deposition density (droplets cm^{-2});

n-number of droplets deposited on the collection substrate (droplets);

S-area of the collection substrate (cm^2).

Droplet deposition was measured using water-sensitive paper. After the experiments, the WSP samples were collected and analyzed using deposition analysis software to obtain droplet number and distribution. The droplet deposition density was then calculated based on the number of droplets per unit area.

Results and Discussion

Determination of optimal wind-shield parameters

Based on the three-factor, three-level orthogonal experiment in Section 2.1, CFD simulations were conducted in ANSYS Fluent for nine hood geometries. Figure 5 presents the resulting discrete-phase droplet trajectories.

Analysis of variance (ANOVA) results (Table 2) reveal the significance of inclination angle θ (°), opening width L (mm), and height H (mm) on drift rate. Here, factors A, B, and C correspond to θ, L, and H, respectively. At $\alpha = 0.05$ (critical value $F_{0.05}(2,2) = 19$), ANOVA yielded $FA < F_{0.05}(2,2)$, $FB > F_{0.05}(2,2)$, and $FC < F_{0.05}(2,2)$. Since FB exceeds the critical value and FC > FA, the results indicate that the hood opening width (L) has a statistically significant effect on drift rate. Furthermore, height H influences drift rate more strongly than angle θ. These findings are consistent with the range-analysis results.

These results indicate that opening width L has the greatest effect on drift rate, followed by height H, which similar to previous research that spray height affected the pesticides' effect (Zhang et al, 2021); the effect of inclination angle θ is not significant at the 1 % level. The optimal hood configuration for maximum drift prevention corresponds to factor-level combination A3B2C1: θ = 80°, opening width L = 1200 mm, and hood height H = 650 mm.

The orthogonal optimization was performed under a constant wind speed of 5 m/s. In addition, identical droplet injection settings were applied in all simulation cases. This ensured that variations in drift rate were solely attributed to differences in hood structural parameters.

Analysis of factors affecting drift

Ambient wind speed and spray pressure critically affect droplet drift during application. Wind speed and spray pressure were selected as independent variables to further evaluate the anti-drift performance of the hood. The displacement of the droplet mass center (D_m) and the drift rate (β_m) were used as evaluation metrics. Table 3 lists the specific levels of ambient wind speed and spray pressure used in the study. Twelve operating conditions were simulated using ANSYS Fluent to quantify the drift-reduction performance of the hood. The values of D_m and β_m were compared for cases with and without the hood under different wind speeds and spray pressures.

During the spraying process, ambient wind speed and spray pressure significantly influence droplet drift. In this study, wind speed and spray pressure were selected as independent variables, while the mass-center displacement (D_m) and drift rate (β_m) were used as evaluation metrics.

The D_m is an important indicator of spray performance. A smaller D_m indicates that droplets remain closer to the nozzle and deposit more effectively in the target region. It is calculated as:

$$D_m = \frac{\sum_{i=1}^{z}(m_i \cdot d_i)}{\sum_{i=1}^{n} m_i} \quad \text{(Eq. 3)}$$

Where:

D_m is the drift mass centroid distance (mm),

i is the droplet index,

z is the total number of droplets,

m_i is the mass of the ith droplet (g),

d_i is the distance between the ith droplet and the nozzle (mm).

The drift rate (βm) is defined as the ratio of the mass of droplets escaping the computational domain to the total sprayed mass, expressed as a percentage. It is calculated as:

$$\beta_m = \frac{M - \sum_{i=1}^{z} m_i}{M} \times 100\% \quad \text{(Eq. 4)}$$

Where:

β_m is the drift rate (%);

m_i is the mass of droplets deposited within the target region (g);

n is the number of deposited droplets;

M is the total sprayed mass (g).

Table 4 compares mass-centroid displacement (Dm) and drift rate (βm) with and without the hood, revealing the following trends: Under constant spray pressure, Dm increases with wind speed, and the difference between hooded and non-hooded cases widens. The smallest displacement difference (4.25 cm) occurs at 2 m/s and 0.2 MPa, while the largest (21.89 cm) occurs at 5 m/s and 0.2 MPa. Under constant wind speed, Dm increases with rising spray pressure.

Table 4 compares drift rates under varying conditions. Under fixed pressure, drift rate increases with wind speed, and the gap between hooded and non-hooded rates widens at higher speeds. The minimum drift-rate reduction (11.5%) occurs at 2 m/s and 0.2 MPa, while the maximum reduction (27.4%) occurs at 4 m/s and 0.4 MPa. Under fixed wind speed, drift rate also increases with rising spray pressure. These simulation results demonstrate that the hood reduces droplet drift by up to 27.4%.

Comparison of anti-drift performance

Each of the four hoods was simulated individually using the airflow-field numerical model established in the previous paragraph. Figure 6 shows the converged continuous-phase velocity fields for six hood configurations. Different hood geometries exert distinct influences on droplet deposition and drift, as follows: hoods (a) and (c) accelerate airflow at both their top and bottom edges. The resulting high-velocity streams drive fine droplets rightward, exacerbating drift and increasing the drift rate. Hood (b) induces a low-velocity recirculation zone downstream, which hinders the deposition of small droplets. Hood (d) generates a high-speed flow region beneath it, promoting droplet deposition and suppressing drift. Its arcuate upper section channels the flow inward, further enhancing performance. Based on the analysis of these flow-field characteristics, the most suitable hood design can be identified to achieve optimal spray deposition with minimal drift. Figure 7 shows the discrete-phase droplet trajectories for six hood configurations, with colors indicating droplet diameter. In Hood (a), droplets smaller than 244 μm drift along the external flow field. In Hood (b), droplets below 227 μm drift, with paths closely following the local velocity vectors. In Hood (c), droplets under 257 μm drift, and a localized recirculation in the right-hand interior induces inward spiraling. Hood (d) markedly reduces droplet drift compared to the other five designs, and shows no significant deposition on the hood surface. Together, these results illustrate that the novel Hood (d) design provides the most effective drift prevention.

Prototype testing of the hooded boom sprayer

The maize–soybean intercropping-specific spray system was installed on a prototype boom sprayer. Off-target drift tests were then conducted for soybean-band and maize-band applications to evaluate the hood's isolation performance under real-world conditions (Figure 8).WSP was placed at the base of non-target plants to collect deposited droplets. Droplet deposition density was then used as the evaluation metric.

With the maize-band spray unit operating, no droplets were detected on the two central soybean rows at any test speed; only the two rows adjacent to the maize unit showed minimal deposition. At 3 km/h, deposition density remained below 1.0 droplets cm^{-2}. As speed increased, edge deposition rose slightly, peaking at 2.1 droplets cm^{-2} at 5 km/h.

With the soybean-band spray unit active, droplet deposition within the maize band remained limited. At the lowest speed, maize-band deposition density ranged from 0.6 to 2.9 droplets cm^{-2}. Although drift rate increased with speed, peak deposition density remained below 8.0 droplets cm^{-2}.

Limitations of the protype experiments and future requirements

Because maize-soybean strip intercropping has not yet entered the seeding, weeding, and chemical-spraying stages, all evaluations of our hooded spray prototype were limited to open-site trials rather than true in-crop field experiments. Consequently, the ambient wind conditions during these tests fluctuated in speed and direction and did not exactly match the uniform 5 m/s inlet boundary used in our CFD simulations, potentially introducing discrepancies in droplet trajectories. The relatively small, obstacle-free test area also prevented assessment of long-distance drift and multi-row interactions typical of operational intercropping systems, and the lack of actual crop canopies omitted their influence on local airflow and deposition patterns. In future work, we will conduct large-scale trials across varied terrains and cropping arrangements, employ wind-tunnel or other controlled-environment facilities to standardize wind parameters, incorporate crops simulants or living plants, explore multiple droplet and agrochemical formulations, and evaluate the long-term operational stability and maintenance requirements of the hooded sprayer design.

Conclusions

This study investigated how wind speed and spray pressure affect the anti-drift performance of hoods. Results show that, with the hood in place, mass-center displacement decreases significantly, and droplet drift reduces by up to 27.4%, with a maximum displacement reduction of 21.89 cm. Field trials were conducted on soybean- and maize-band spray units to evaluate the drift-prevention performance of the hoods, showing good agreement with CFD predictions. Airflow patterns and droplet trajectories for four hood designs were also simulated using deposition and drift rates as evaluation metrics. These analyses confirmed that the novel hood developed here delivers the best anti-drift performance. Finally, prototype experiments at varying forward speeds measured cross-band deposition, further validating that the designed hood meets the agronomic requirements of maize-soybean strip intercropping systems.

References

Ahmad F, Zhang S, Qiu B, Ma J, Xin H, Qiu W, et al., 2022. Comparison of water sensitive paper and glass strip sampling approaches to access spray deposit by UAV sprayers. Agronomy 12:1302.

Baetens K, Nuyttens D, Verboven P, De Schampheleire M, Nicolaï B, Ramon H, 2007. Predicting drift from field spraying by means of a 3D computational fluid dynamics model. Comput Electron Agr 56:161-173.

Cortez JW, Furlani CEA, da Silva RP, Arcoverde SNS, 2018. Performance of corn sowing in fertilization system and intercropping. Eng Agric 38:225-231.

Cui G, Sun X, Liu J, Shi Y, Li J, Li Y, et al., 2023. Design and test of boom sprayer for strip compound planting mode of soybean and maize. J Henan Agri Univ 57:752-763.

Cunha JPAR, dos Reis EF, de Assunção HHT, Landim TN, 2019. Evaluation of droplet spectra of the spray tip AD 11002 using different techniques. Eng Agric 39:476-481.

Dong F, He W, Zhou HP, 2023. Numerical simulation and experimental analysis of spray field of impingement nozzle. Eng Agric 43:1-10.

Dong X, Li Z, Ou M, Jia W, 2025. Design and Exploitation of a dual-channel direct injection system. Agriculture 15:1029.

Hu Y, Chen Y, Wei W, Hu Z, Li P, 2021. Optimization design of spray cooling fan based on cfd simulation and field experiment for horticultural crops. Agriculture 11:566.

Kama R, Liu Y, Aidara M, Kpalari DF, Song J, Diatta S, et al., 2024. Plant-soil feedback combined with straw incorporation under maize/soybean intercropping increases heavy metals migration in soil-plant system and soil HMRG abundance under livestock wastewater irrigation. J Soil Sci Plant Nut 24:7090-7104.

Kong F, Qiu B, Dong X, Yi K, Wang Q, Jiang C, et al., 2024. Design and development of a side spray device for UAVs to improve spray coverage in obstacle neighborhoods. Agronomy 14:2002.

Laguardia AFB, Fajardo AL, Zubia OF, Valencia RC, Gallegos RKB, 2023. Determination of spray drift characteristics of a Ronnie Baugh tractor-trailed boom sprayer using computational fluid dynamics. Eng Agric 43:1-14.

Li C, Hoffland E, Kuyper TW, Yu Y, Zhang C, Li H, et al., 2020. Syndromes of production in intercropping impact yield gains. Nat Plants 6:653-660.

Li H, Travlos I, Qi L, Kanatas P, Wang P, 2019. Optimization of herbicide use: study on spreading and evaporation characteristics of glyphosate-organic silicone mixture droplets on weed leaves. Agronomy 9:547.

Li S, Li J, Yu S, Wang P, Liu H, Yang X, 2023. Anti-drift technology progress of plant protection applied to orchards: a review. Agronomy 13:2679.

Liu C, Hu J, Chu X, Li Y, Sun S, Zhang W, 2021. [Optimization of the inner flow channel of conical wind field anti-drift spray device and anti-drift characteristics].[Article in Chinese with English abstract]. T CSAE 37:11-20.

Liu W, Chen X, Zeng S, 2024. Design and parameter optimization of a rigid-flexible coupled rod tooth threshing device for ratoon rice based on MBD-DEM. Agriculture 14:2083.

Moore VM, Schlautman B, Fei S, Roberts LM, Wolfe M, Ryan MR, et al., 2022. Plant breeding for intercropping in temperate field crop systems: a review. Front Plant Sci 13:843065.

Nuyttens D, De Schampheleire M, Baetens K, Sonck B, 2007. The influence of operator-controlled variables on spray drift from field crop sprayers. T ASABE 50:1129-1140.

Ozkan H, Miralles A, Sinfort C, Zhu H, Fox R, 1997. Shields to reduce spray drift. J Agr Eng Res 67:311-322.

Padalkar G, Mandlik R, Sudhakaran S, Vats S, Kumawat S, Kumar V, et al., 2023. Necessity and challenges for exploration of nutritional potential of staple food grade soybean. J Food Compos Anal 117:105093.

Qin W, Xue X, Cui L, Zhou Q, Xu Z, Chang F, 2016. Optimization and test for spraying parameters of cotton defoliant sprayer. Int J Agr Biol Eng 9:47-54.

Tang P, Li H, Issaka Z, Chen C, 2017. Impact forces on the drive spoon of a large cannon irrigation sprinkler: simple theory, CFD numerical simulation and validation. Biosyst Eng 159:1-9.

Tsay J, Fox R, Ozkan H, Brazee R, Derksen R, 2002. Evaluation of a pneumatic-shielded spraying system by CFD simulation. T ASAE 45:47-54.

Tu J, Guan H, Liu C, 2019. Computational fluid dynamics - A practical approach. 3rd ed. Oxford, Butterworth-Heinemann.

Wei XP, 2021. CFD simulation and experiment of shields spray system. Degree Diss., Northwest A&F University, China.

Wu Y, Wang E, Gong W, Zhao Z, He D, Yang F, et al., 2023. Soybean yield variations and the potential of intercropping to increase production in China. Field Crop Res 291:108771.

Yu Y, Wang G, Tang Z, Cao Y, Zhao CY, 2023. Structural form and field operation effect of crawler type broccoli harvester. Eng Agric 43:1-18.

Zhang S, Qiu B, Xue X, Sun T, Gu W, Zhou F, et al., 2021. Effects of crop protection unmanned aerial system flight speed, height on effective spraying width, droplet deposition and penetration rate, and control effect analysis on wheat aphids, powdery mildew, and head blight. Appl Sci 11:712.

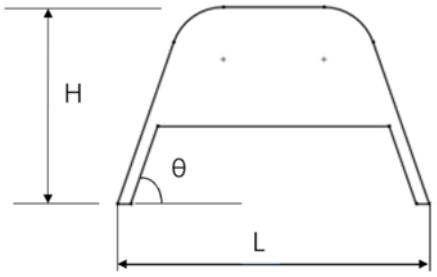

Figure 1. Dimension of the hood structure.

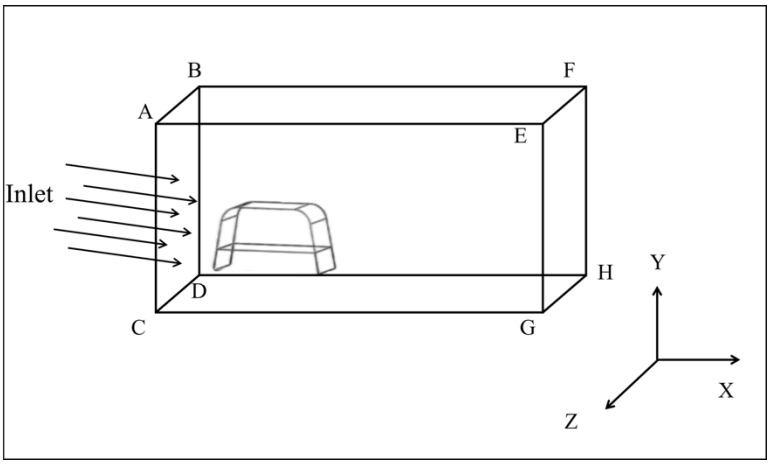

Figure 2. Three-dimensional model of the airflow field.

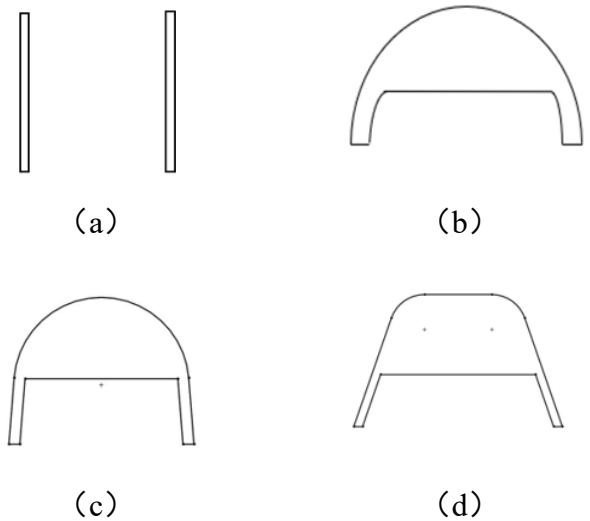

Figure 3. Model diagrams of the four hoods design.

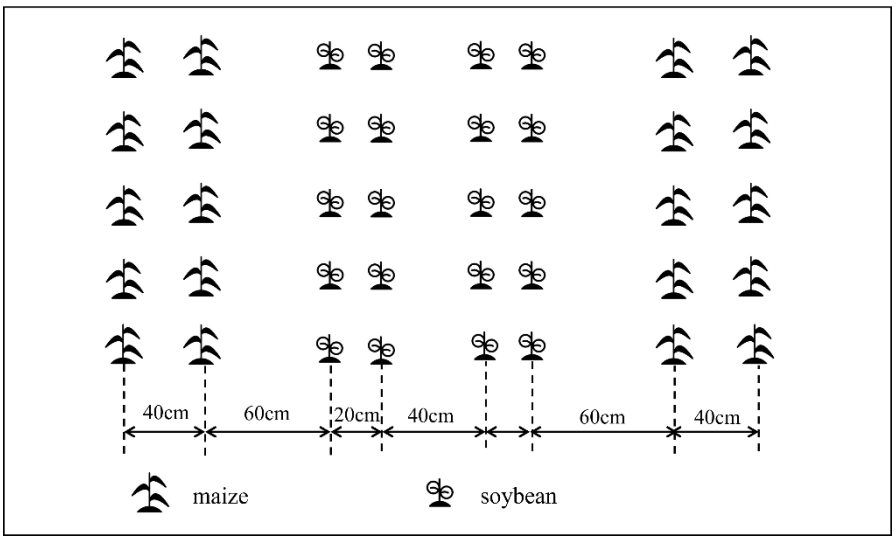

Figure 4. Maize-soybean simulation model.

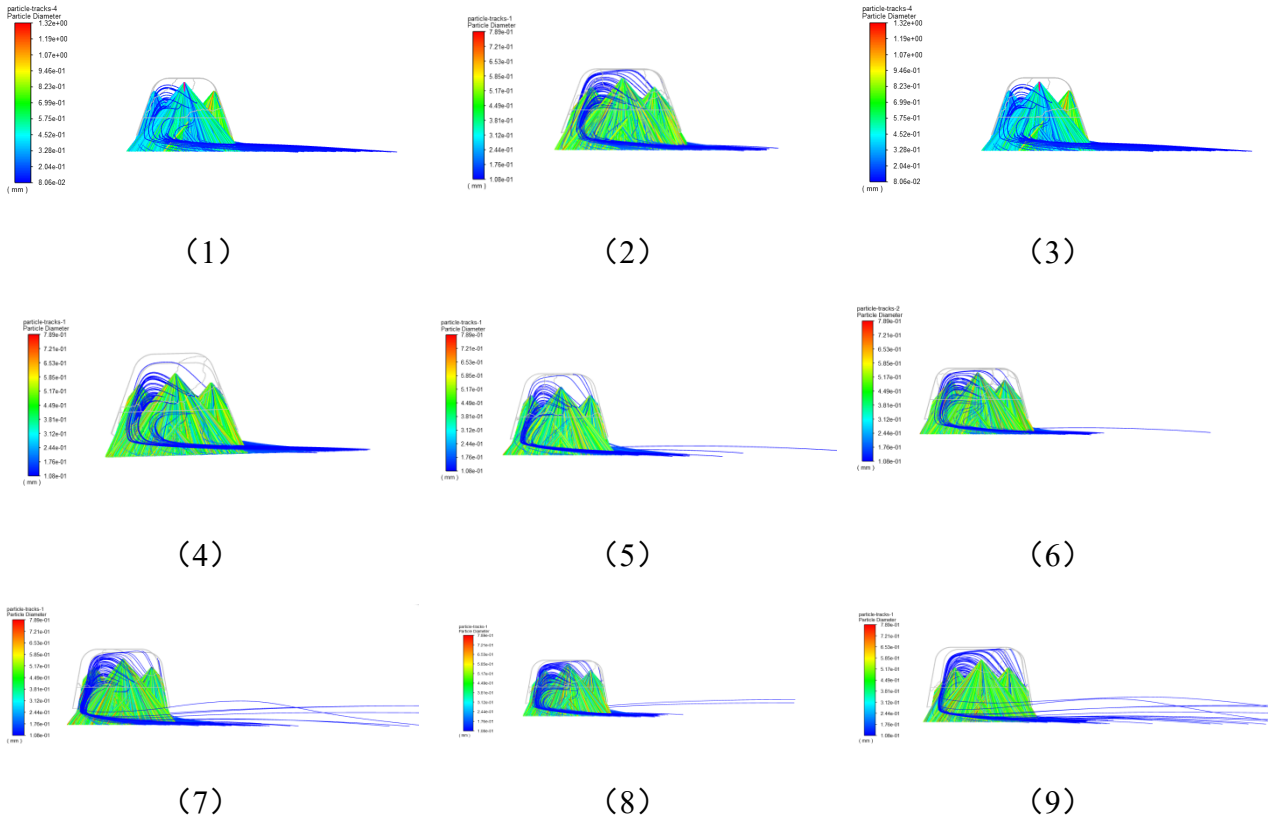

Figure 5. Discrete-phase droplet trajectories for wind shields of different dimensions.

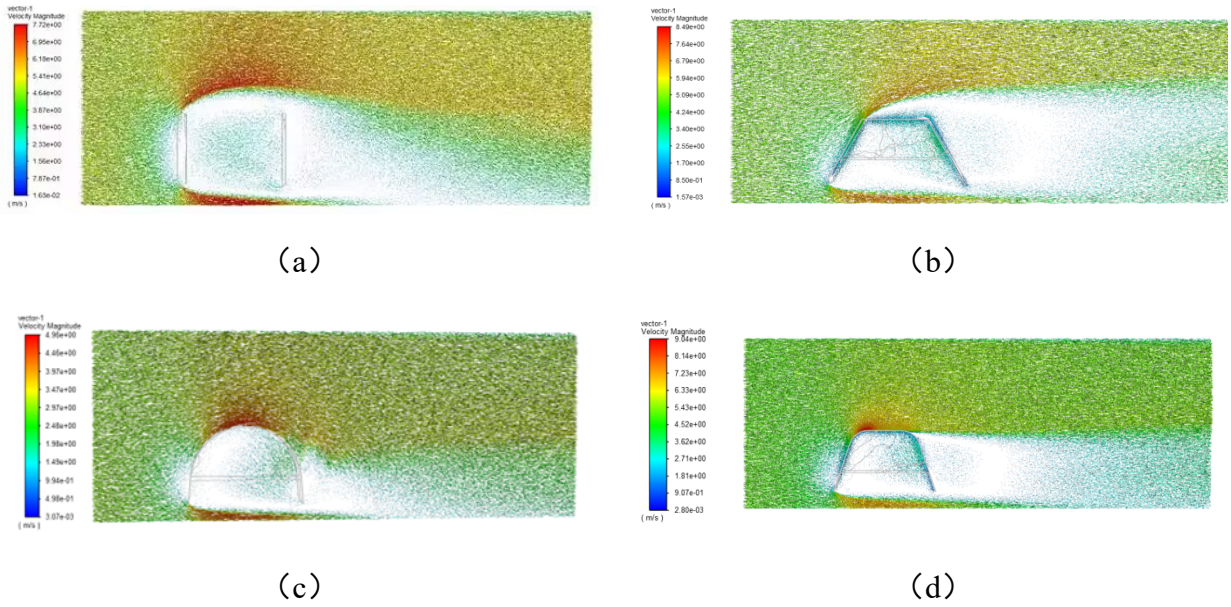

Figure 6. Flow distribution of the airflow fields for the four wind-shield designs.

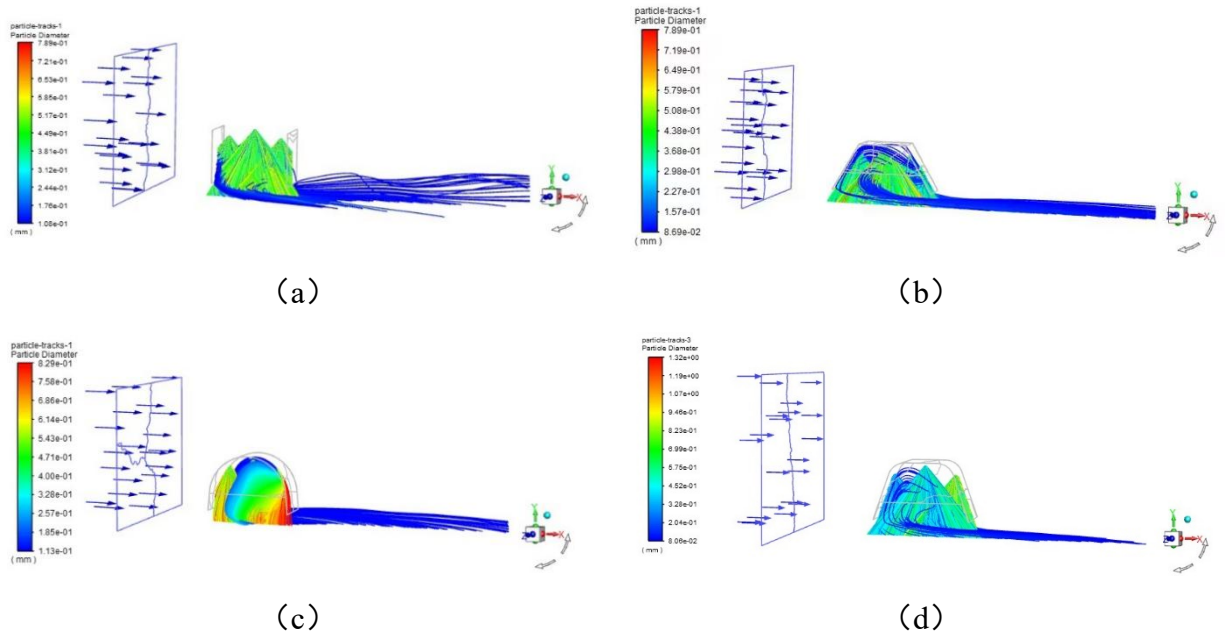

Figure 7. Discrete-phase droplet trajectories for various wind-shield designs.

Figure 8. Anti-drift experiment protype.

Table 1. Factor level table.

Level	θ (°)	L (mm)	H (mm)
1	70	1100	650
2	75	1200	700
3	80	1300	750

Table 2. Analysis of variance for drift-rate factors.

Source	Sum of Squares	degree of freedom	Mean Square	F-value	Significance
θ (°)	6.805	2	3.403	1.977	*
L (mm)	73.765	2	36.882	21.432	***
H (mm)	18.220	2	9.110	5.294	**
Error	3.442	2	1.721	-	-
Total	102.232	8	-	-	-

Table 3. Factor level table for drift analysis.

Factor	Levels
Wind speed (m/s)	2,3,4,5
Spray pressure (MPa)	0.2,0.3,0.4

Table 4. Simulation results of center distance and drift rate.

Number	Wind speeds (m/s)	Pressure (Mpa)	Hoods spray		Without hoods spray	
			D_m (cm)	β_m (%)	D_m (cm)	β_m (%)
1	2	0.2	0.48	0.0	4.73	11.5
2	2	0.3	1.41	1.5	7.36	22.3
3	2	0.4	3.93	3.5	8.39	19.2
4	3	0.2	1.07	2.7	11.32	20.3
5	3	0.3	3.01	4.3	10.55	18.7
6	3	0.4	6.73	6.5	13.66	22.9
7	4	0.2	2.07	4.1	19.64	26.8
8	4	0.3	4.11	6.3	17.82	23.2
9	4	0.4	9.28	9.8	20.39	37.2
10	5	0.2	4.95	9.3	26.84	29.9
11	5	0.3	9.12	15.2	26.37	34.0
12	5	0.4	11.4	22.5	29.45	38.8